Department of Biochemistry[1], School of Medicine, University of Patras; Department of Biochemistry and Biotechnology[2], University of Thessaly, Larissa, Greece

Clindamycin binding to ribosomes revisited: foot printing and computational detection of two binding sites within the peptidyl transferase center

O. N. Kostopoulou[1], G. Papadopoulos[2], E. C. Kouvela[1], D. L. Kalpaxis[1]

Received October 12, 2010, accepted December 10, 2012

Prof. Dr. Dimitrios Kalpaxis, Department of Biochemistry, School of Medicine, University of Patras, 26504 Patras, Greece
dimkal@med.upatras.gr

Dedicated to Prof. Dr. Theo Dingermann, Frankfurt, on the occasion of his 65th birthday.

Pharmazie 68: 616–621 (2013) *doi: 10.1691/ph.2013.6508*

Clindamycin is a semi-synthetic lincosamide, active against most Gram-positive bacteria and some protozoa. It binds to the 50S ribosomal subunit and inhibits early peptide chain elongation. By kinetic analysis it has been shown that clindamycin (I) competitively interacts with the A-site of translating ribosomes (C) to form the encounter complex CI, which then slowly isomerizes to a tighter complex, termed C*I. As the final complex is capable of synthesizing peptide bonds with decreased velocity, it was assumed that in C*I complex the drug is fixed near the P-site of the ribosome. In the present study, two series of chemical foot printing experiments were carried out. In the first series, clindamycin and ribosomal complex C were incubated for 1 s and then DMS or kethoxal was added (CI probing). In the second series, complex C was preincubated with clindamycin for 1 min before the addition of DMS or kethoxal (C*I probing). It was found that clindamycin in CI complex protects A2451 and A2602 from chemical probing, both located within the A-site of the catalytic center. In contrast, it strongly protects G2505 in C*I complex, which is a discrete foot print of peptidyl-tRNA bound to the P-site. In both CI and C*I complexes, clindamycin also protects nucleotides A2058 and A2059, located next to the entrance of the exit-tunnel where the nascent peptide leaves the ribosome. Polyamines negatively affect the protection of G2505, but favor the protection of A2451 and A2602 nucleotides. Structure modeling confirms the kinetic and chemical foot printing results and suggests that clindamycin mode of action is more complex than a simple competitive inhibition of peptide bond formation.

1. Introduction

Ribosomes, the subcellular organelles where protein synthesis takes place, are the major target for natural and synthetic antibiotics. Complexes of ribosomal subunits with antibiotics are essential to understand the molecular mechanism of antibiotic action and resistance.

The peptidyl transferase (PTase) center of the ribosome is inhibited by many groups of antibiotics including lincosamides (Wilson 2009). Clindamycin is a semi-synthetic derivative of lincomycin (7(*S*)-chloro-7-deoxylincomycin, Fig. 1) and is active against most Gram-positive bacteria and some protozoa. It belongs to the MLS_B (macrolides, lincosamides, $streptogramins_B$) antibiotics which although structurally diverse, all share an overlapping binding site in 23S rRNA of the 50S subunit of bacterial ribosome (Roberts et al. 2008). Crystallographic studies have shown that the propyl pyrrolidinyl tail of clindamycin occupies the same ribosomal cleft as the O-methyl tyrosine residue of the A-site pseudo-substrate CC-puromycin (Schlünzen et al. 2001; Tu et al. 2005; Dunkle et al. 2010), while its galactose group interacts with a ribosomal site occupied by the desosamine sugar of macrolides. Nevertheless, chemical foot printing analysis (Douthwaite et al., 1992), resistance analysis (Triman 1999; Kehrenber et al. 2005; Poehlsgaard et al. 2005), and molecular modeling approaches (Cheney 1974; Fitzhugh 1998) have proposed that clindamycin interferes with the positioning of aminoacyl moieties of tRNAs at both A-site and P-site on the 50S ribosomal subunit. In agreement with earlier binding studies investigating the competition of lincosamides on the binding of 3′terminus tRNA fragments from *N*-Acetyl(Ac)Leu-$tRNA^{Leu}$, Leu-$tRNA^{Leu}$ and Phe-$tRNA^{Phe}$ to the P-site (Celma et al. 1970; Černá and Rychlík

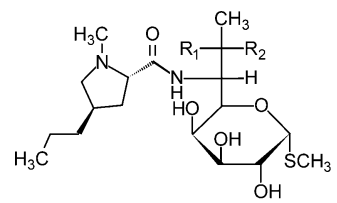

Fig. 1: Chemical structures of clindamycin (R1 = H, R2 = Cl) and lincomycin (R1 = OH, R2 = H).

1972), recent kinetic studies revealed that clindamycin, after a transient interference with the A-site of ribosomes, slowly shifts towards the P-site and perturbs the PTase center, so that a peptide bond is still formed but with a lower catalytic rate constant compared with that measured in the absence of the drug (Kouvela et al. 2006). Data from the same study demonstrated that polyamines exhibit an overall, beneficial effect on clindamycin's potency. Although these polycations negatively affect the binding to the P-site, they exert a positive, more pronounced effect on the binding of clindamycin to the A-site complex (Kouvela et al. 2006).

Despite considerable interest in unraveling the clindamycin interaction with ribosomes by crystallography, these studies provided only a snapshot of the clindamycin binding process and could not describe the entire course of the drug interaction with the ribosome. In addition, most of these studies have been performed in buffer systems that are far from the physiological ionic environment of the cell. However, it has been documented that monovalent and divalent ions, as well as polyamines are essential components for the PTase activity and the binding of lincosamides to the ribosome (Vogel et al. 1971; Kallia-Raftopoulos et al. 1994; Kouvela et al. 2006). Nevertheless, binding and kinetic studies, while revealing the functional consequences of clindamycin binding to ribosomes, cannot dissect the unique conformations and spatial interactions by which the drug gains access to the ribosome. Therefore, the binding of clindamycin to ribosomes needs to be further investigated, using additional experimental approaches.

In the present study, time-resolved foot printing analysis is applied to investigate the entire course of clindamycin interaction with *Escherichia coli* functional ribosomal complexes, under various ionic conditions. Combined with molecular modeling analysis, our results solve previous uncertainties and offer new clues about how clindamycin detects its binding position in the ribosome and how polyamines affect this binding.

2. Investigations and results

As previously indicated (Kouvela et al. 2006), clindamycin binds to a complex of poly(U)-programmed ribosomes from *E. coli*, complex C, bearing $tRNA^{Phe}$ at the E-site and AcPhe[^{3}H]$tRNA^{Phe}$ at the P-site in buffer 4.5 mM Mg^{2+} and 150 mM NH_4^+, in a two-step process according to the kinetic scheme:

$$C + I \underset{}{\overset{K_i}{\rightleftarrows}} CI \underset{k_7}{\overset{k_6}{\rightleftarrows}} C^*I$$

The encounter complex CI is established instantaneously, while the isomerization step is slowly accomplished. The apparent association rate constant of binding $(k_6+k_7)/K_i$ is equal to 6.33×10^4 $M^{-1}s^{-1}$, a value considerably lower than the upper limit set for the characterization of an antibiotic as a slow binding inhibitor (Morrison and Walsh 1988).

In order to identify the individual drug-ribosome interactions occurring in the encounter complex CI and the final complex C*I, two series of experiments were carried out. In the first, clindamycin and complex C were allowed to react at 25 °C (rapid formation of CI complex) and simultaneously incubated with chemical reagents modifying susceptible nucleotides in 23S rRNA, except for those participated in drug binding. It is important to mention that the used chemicals react with accessible nucleotides in a few milliseconds (Fabbretti et al. 2007). In the second series, 100 nM complex C were preincubated with 55 μM clindamycin for 1 min before adding DMS or kethoxal. That means, that in order to foot print the C*I complex, the incubation time of complex C with clindamycin was extended

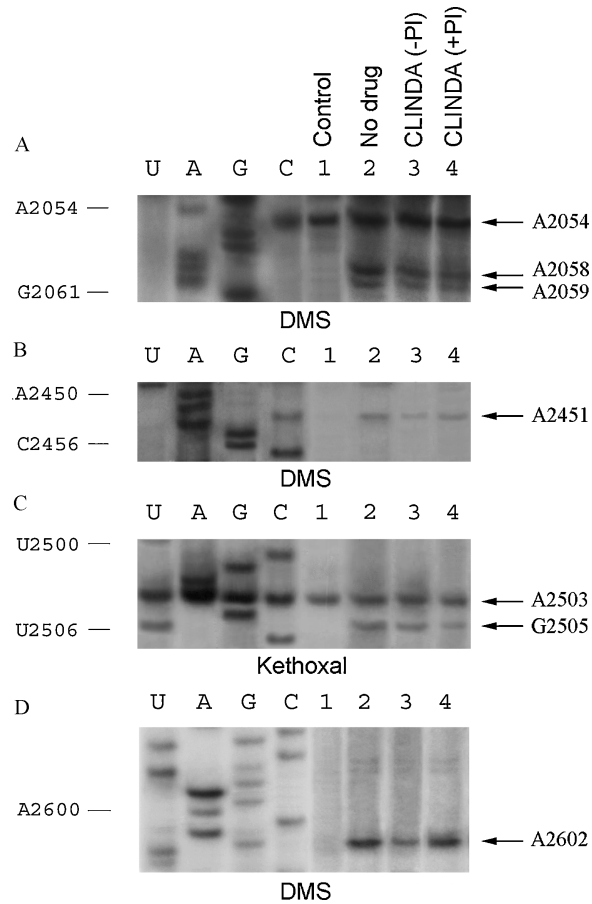

Fig. 2: Protections against chemical probes in nucleotides of the central loop of domain V of 23S rRNA, caused by clindamycin binding to complex C. Antibiotic binding was performed practically without preincubation (-PI) or with preincubation for 1 min (+PI) in buffer B. The resulting complexes were then probed with DMS or kethoxal. The modification sites were detected by primer extension analysis. U, A, G and C are dideoxy sequencing lanes. Lane 1, untreated complex C; lane 2, complex C probed in the absence of clindamycin; lane 3, complex C reacting with clindamycin for 1 s and then probed; lane 4, complex C reacting with clindamycin for 1 min and then probed. Numbering of nucleotides for the sequencing lanes is shown at the left. AMV reverse transcriptase stops or pauses are indicated by arrows at the right. AMV reverse transcriptase halts one position before a modified nucleotide.

to more than ten half lives ($t_{1/2}$). The value of $t_{1/2}$ was calculated by Eq. (1)

$$t_{1/2} = \frac{0,693}{k} \tag{1}$$

where k is the apparent equilibration rate constant given by Eq. (2)

$$k = k_7 + k_6 \frac{[I]}{[I] + K_i} \tag{2}$$

The time ($10 \times t_{1/2}$) till the equilibrium between complex C and the drug did not exceed the value of 4.6 s, at either ionic conditions examined. On the other hand, the isomerization constant k_6/k_7 was at least 7.2. Therefore, at the end of 1 min more than 88% of complex C was part of complex C*I.

Monitoring of modifications in 23S rRNA were performed by primer extension analysis. Representative autoradiograms are shown in Figs. 2 and 3. The final modification results are summarized in the Table. When complex C reacted with clindamycin for a short time period, protection was observed mainly at nucleotides A2451 and A2602 (Fig. 2). In contrast, when complex C was preincubated with clindamycin for 1 min and then modified by the chemical probe, strong protection was

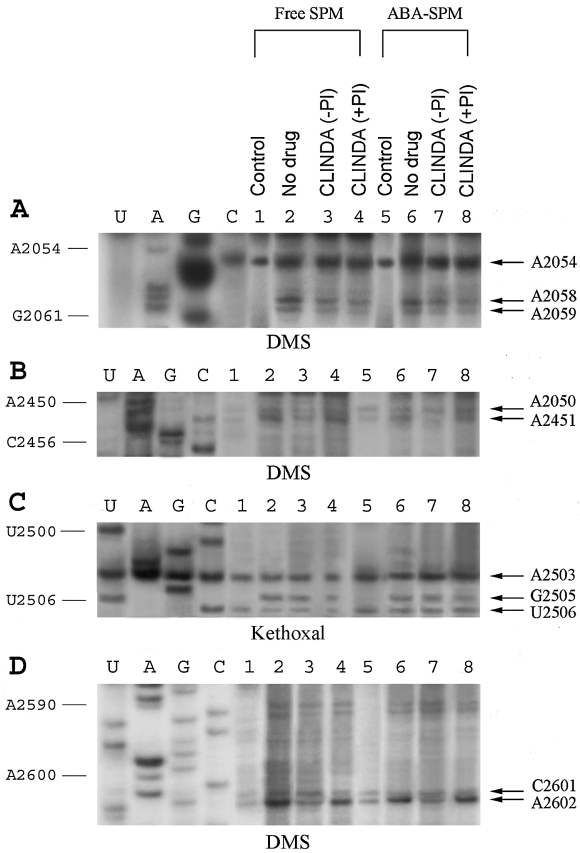

Fig. 3: Protections against chemical probes in nucleotides of the central loop of domain V of 23S rRNA, caused by clindamycin binding to complex C in the presence of spermine free or covalently bound to complex C. Antibiotic binding was performed in buffer B containing 100 μM spermine and 100 nM complex C (lanes 1-4) or in buffer B containing 100 nM complex C photolabeled with 100 μM ABA-spermine (lanes 5-8). The resulting complexes were then probed with DMS or kethoxal. The modification sites were detected by primer extension analysis. U, A, G and C are dideoxy sequencing lanes. Lanes 1 and 5, non probed ribosomal complex; lanes 2 and 6, ribosomal complex probed in the absence of clindamycin; lanes 3 and 7, ribosomal complex reacting with clindamycin for 1 s and then probed; lanes 4 and 8, ribosomal complex reacting with clindamycin for 1 min and then probed. Numbering of nucleotides for the sequencing lanes and AMV reverse transcriptase stops or pauses are indicated as in Fig. 2.

observed only at nucleotide G2505. In both cases, clindamycin also protected nucleotides A2058 and A2059, clustered around a hydrophobic interstice positioned at the entrance of the tunnel where the nascent peptide leaves the ribosome (Fig. 2). Addition of spermine favored the protection of A2451 and A2602 in complex CI, but reduced the protection of G2505 in C*I (Fig. 3). The band corresponding to A2503 is probably due to a methylation of 23S rRNA at the adenine base (Kehrenberg et al. 2005), while the band at A2054, also presented in the control lane, may be related to a nonspecific pause in reverse transcription. Similar results to those obtained in the presence of spermine were achieved, when complex C was photolabeled with ABA-spermine, except for protections concerning nucleotides susceptible to the photoprobe (e.g. A2450, U2506, and C2601).

Tempted by the fact that two out of three possible conformations of clindamycin, when bound to the ribosome, show significant differences (Schlünzen et al. 2001; Tu et al. 2005; Dunkle et al. 2010), a clindamycin-ribosome modeling system was used to explain the different foot printing pattern between CI and C*I complexes. The system was based on the structure of the *E. coli* 50S ribosomal subunit (PDB: 3OFZ). A- and P-site bound tRNAs from *Thermus thermophilus* (PDB: 2WDK) were introduced into the scene, after structural alignment of *E. coli* and *T. thermophilus* 50S subunits using the program

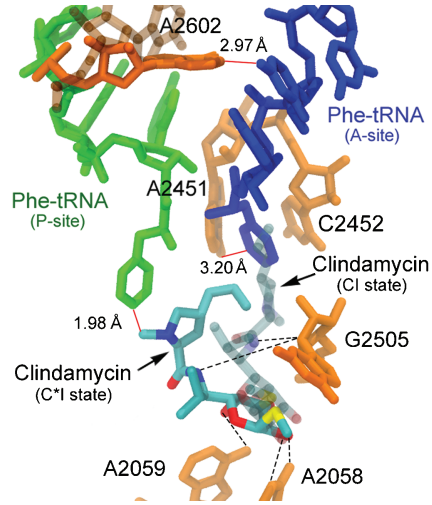

Fig. 4: Binding position of clindamycin on the *E. coli* ribosome, as detected by molecular docking of the drug into the 50S ribosomal subunit from *E. coli* (PDB: 30FC), starting from two different poses. A- and P-site bound Phe-tRNAs (colored blue and green, respectively) have been introduced in the model after structural alignment of *E. coli* and *T. thermophilus* 50S subunits (PDB: 2WDK) using the program VMD. Nucleotide A2602 is shown in two orientations; one taken from native *E. coli* 50S ribosomal subunits (Dunkle et al. 2010), colored brown, and a second one taken from CCA-puromycin bound to 50S ribosomal subunits from *D. radiodurans* (Bashan et al. 2003), colored orange. Hydrogen bonds are shown as black dashes, while distances between certain residues are indicated by red lines.

VMD (Humphrey et al. 1996). When docked into the modeling system, clindamycin bearing a conformation like that detected in an *E. coli* ribosome-clindamycin complex by crystallography (Dunkle et al. 2010), was found to be engaged in most of the hydrogen bonding and van der Waals interactions with 23S rRNA, derived by this crystallographic study. The model is in good agreement with the foot printing pattern of CI complex. Steric clashes are minimal, and the only major overlap is between the pyrrolidinyl moiety of clindamycin and the aminoacyl tail of tRNA bound to the A-site (Fig. 4; Clindamycin-CI state). In crystals of ribosome-clindamycin from *Deinococcus radiodurans* (Schlünzen et al. 2001) another conformation of clindamycin was found with the propyl pyrrolidinyl group rotated by 180° in relation to the plane of the galactose ring. Using this conformation for the docking model leads to a new orientation of the drug within the binding pocket, which reveals a new putative hydrophobic interaction between the propyl-pyrrolidinyl group and the aminoacyl moiety of tRNA bound to the P-site (Fig. 4; Clindamycin-C*I state). This model is more consistent with the foot printing pattern of C*I complex and provides an explanation how clindamycin may allow complex C*I to react with puromycin, albeit with lower catalytic efficiency than complex C.

3. Discussion

Knowledge on the binding of an antibiotic to its molecular target is a prerequisite to understand its mechanism of action. Notwithstanding effort for shedding light on the clindamycin binding to ribosomes, we are still unable to conceive the implication of this knowledge, given that results from different groups disagree about the exact binding site, while others suggest different conformations of clindamycin bound to the ribosome. A recent study analyzing the structure of clindamycin-ribosome from *E. coli* seems to address the disagreements between earlier crystallographic studies (Dunkle et al. 2010), but still fails to completely verify previous binding and kinetic results.

A kinetic study recently showed that clindamycin behaves as a slow binding inhibitor of peptide-bond formation, following a

Table: Foot printing of the clindamycin binding sites in the central loop of Domain V of 23S rRNA, at the initial (CI) and the final (C*I) binding states[a]

23S rRNA residue	Ionic conditions								
	4.5 mM Mg^{2+}, 150 mM NH_4^+			4.5 mM Mg^{2+}, 150 mM NH_4^+ 100 μM spermine			4.5 mM Mg^{2+}, 150 mM NH_4^+ 100 μM ABA-spermine		
	C	CI	C*I	C	CI	C*I	C	CI	C*I
A2058	1	0.69 ± 0.07^b	0.54 ± 0.05^b	1	0.72 ± 0.08^b	0.72 ± 0.07^b	1	0.73 ± 0.08^b	0.73 ± 0.07^b
A2059	1	0.80 ± 0.09^b	0.77 ± 0.08^b	1	0.78 ± 0.08^b	0.85 ± 0.07^b	1	0.80 ± 0.08^b	0.85 ± 0.08^b
A2451	1	0.62 ± 0.05^b	$0.78 \pm 0.07^{b,c}$	1	0.48 ± 0.06^b	0.69 ± 0.08^c	1	0.56 ± 0.07^b	0.70 ± 0.08^c
G2505	1	0.87 ± 0.08^b	$0.35 \pm 0.06^{b,c}$	1	0.89 ± 0.08	0.54 ± 0.04^b	1	0.90 ± 0.07	0.50 ± 0.07^b
A2602	1	0.53 ± 0.07^b	0.98 ± 0.08	1	0.39 ± 0.08^b	1.00 ± 0.08^c	1	0.40 ± 0.04^b	0.94 ± 0.08^c

[a] Each relative reactivity of nucleotides shown in the table denotes the ratio between the intensity of a band of interest and the intensity of the corresponding control band (complex C).
[b] Significantly different in relation to C, for the same ionic conditions ($P < 0.05$); [c] Significantly different in relation to CI, for the same ionic conditions ($P < 0.05$).

two-step mechanism (Kouvela et al. 2006). According to this study, and in agreement with transferred nuclear Overhauser effect (TRNOE) spectroscopy (Verdier et al. 2000), clindamycin instantaneously reacts with a post-translocation ribosomal complex (C) to form the encounter complex CI, which then slowly isomerizes to a final complex, C*I. While clindamycin and puromycin are mutually exclusive in the first step of binding, C*I complex is reactive towards puromycin, although 34-fold less than complex C. This implies that at the first step of binding clindamycin competes with the substrate for the ribosomal A-site, while in complex C*I it affects the P-site. Nevertheless, a kinetic analysis cannot directly unravel the structural details by which the drug gains access to the ribosome. Here, we characterize the binding site of clindamycin in the ribosome under various ionic conditions by time-resolved foot printing analysis and combine the obtained data with molecular modeling to define the conformations and contacts of the drug within the ribosomal binding pocket.

Time-resolved foot printing analysis is based on the fact that complex CI is instantaneously formed, whereas the subsequent isomerization of CI to C*I proceeds slowly. During an incubation period of one second, high concentration of clindamycin ($10 \times K_i$) strongly shifts the equilibrium of $C + I \rightleftharpoons CI$ to the right, with 90% of complex C being in the form of complex CI. Meanwhile, less than 25% of CI is converted to C*I. Therefore, at the end of the time period of one second, the incubation mixture should be enriched in CI. In contrast, by incubating complex C with clindamycin for one minute ($30 \times t_{1/2}$), more than 88% of complex C should be in the conformation of C*I. The foot printing data of clindamycin binding at the initial step (complex CI) showed that drug binding strongly reduces the accessibility of nucleotides A2451, A2602 and A2058 to DMS, whereas A2059 and G2505 are still accessible. The first two nucleotides are referred to as "inner shell" PTase nucleotides (Youngman et al. 2004) and both are strongly protected by aminoacyl-tRNA bound to the ribosomal A-site (Moazed and Noller 1989). Thus, clindamycin in CI complex likely interferes with substrate binding to the A-site, in agreement with the conclusions drawn by kinetic studies (Kouvela et al. 2006). Nucleotides A2058, A2059, and G2505 participate in the binding of macrolides and ketolides, and this fact explains why clindamycin share cross-resistance mutations with these antibiotics (Triman 1999). The protection pattern of CI correlates well with foot printing data obtained by others (Douthwaite 1992; Kehrenberg et al. 2005), as well as with crystallographic findings (Schlünzen et al. 2001; Dunkle et al. 2010), except for the absence of protection at A2503 and the appearance of a new protection at A2602. It should be mentioned that a strong stop of reverse transcriptase at A2504, seen also in the control lane of the autoradiograms (Fig. 2), may have artificially concealed possible protection effects on A2503. With regards to A2602, this nucleotide is located at the center of the PTase cavity and adopts various orientations dependent on the functional state of the ribosome and the nature of the bound substrates. It has proposed by Agmon et al. (2004) that A2602 is a candidate element of the ribosomal catalytic center for repositioning of transiently bound substrate analogs. Therefore, interaction of clindamycin with A2602 may be an early and transient event that disappears during the subsequent isomerization of CI to C*I. It is noteworthy that previous foot printing and crystallographic analyses have been performed with high concentrations of clindamycin (0.1 to 1000 μM), for prolonged time (30 min), which bypass the formation of CI complex.

Accommodation of clindamycin at its final position eliminates the contact with A2602 and weakens the interaction with A2451, but retains drug interactions with A2058 and A2059 and favors contacts with G2505 (Table). The foot printing pattern of C*I better resembles the model published by Douthwaite (1992). Nevertheless, the stronger protection at G2505 compared to that seen in CI complex implies that during the isomerization step $CI \rightleftharpoons C^*I$ clindamycin is moved towards the P-site, occupying an intermediate space between A- and P-sites from which it affects the stability and reactivity of P-site bound peptidyl-tRNA. Since protections at A2058 and A2059 are seen in both CI and C*I complexes, we assume that the galactose sugar remains at essentially the same position during this moving, while the propyl-pyrrolidinyl moiety rotates to end up in a new ribosomal environment.

Based on foot printing results of the present study, a model of clindamycin binding to *E. coli* ribosomes was derived, by applying molecular docking techniques and using two starting conformers of clindamycin differing in the relative orientation of the galactose and propyl-pyrrolidinyl rings. In addition, two Phe-tRNAs bound at the A- and P-sites of *T. thermophilus* ribosomes were introduced in the model, after structural alignment of *E. coli* and *T. thermophilus* 50S ribosomal subunits. When the first conformer of clindamycin, resembling that proposed by Dunkle et al. (2010), is docked into the binding pocket, the pyrrolidinyl moiety overlaps the phenylalanyl portion of the A-site bound tRNA, while the rest of the clindamycin molecule adopts numerous interactions with nucleotides of the PTase cavity, all consistent with the foot printing pattern of CI complex (Fig. 4; clindamycin-CI state). The serious clash of pyrrolidinyl moiety with the aminoacyl end of the A-site bound tRNA concurs with the kinetic evidence that clindamycin behaves as a competitive inhibitor of peptide-bond formation within the CI complex. When clindamycin is docked into the binding pocket with the pyrrolidinyl ring rotated relative to the galactose ring, the propyl-pyrrolidinyl moiety shifts towards the P-site (Fig. 4; clindamycin-C*I state). At this position, clindamycin

stops to strongly interfere with the A-site and, as approaching the P-site, causes a disturbance in the functional orientation of the peptidyl tail of the P-site bound tRNA. This position of clindamycin is consistent with the footprinting pattern of C*I complex and explains why clindamycin allows C*I complex to exhibit low activity against puromycin (Kouvela et al. 2006) and why it causes dissociation of short peptidyl-tRNAs (Menninger and Coleman, 1993; Tenson et al. 2003). It is plausible, that modifications in the propyl-pyrrolidinyl group could limit the flexibility of this moiety and/or offer better accessibility to the P-site, thus improving the pharmaceutical properties of the drug.

The presence of spermine in the reaction mixture, free or covalently bound to complex C, strengthens the protection of A2451 and A2602 in complex CI, but ameliorates the accessibility of G2505 to kethoxal in complex C*I (Fig. 3). These results confirm kinetic evidence, according to which polyamines exert a negative effect on the isomerization of CI to C*I, but a positive and more pronounced effect on the formation of CI (Kouvela et al. 2006). As indicated previously, spermine is capable of binding to ribosomal residues, e.g. A2450, A2451, U2506, and A2602, implicated in clindamycin accommodation (Xaplanteri et al. 2005). It has been hypothesized that spermine induces changes in the ribosomes which may reduce the entropic cost of clindamycin binding (Kouvela et al. 2006).

In conclusion, our data confirm previous binding and kinetic evidence that clindamycin affects both the A- and P-sites of the ribosome, due to the flexibility of its propyl-pyrrolidinyl group, and that polyamine influence the binding mode of the drug. From a pharmaceutical point of view, the description of the entire course of clindamycin binding to the ribosome provides avenues for drug modifications to develop new clindamycin analogs with improved potency.

4. Experimental

4.1. Reagents and materials

Spermine tetrahydrochloride, clindamycin, $tRNA^{Phe}$ from *E. coli*, dimethyl sulfate (DMS), kethoxal and DMS stop solution were supplied by Sigma. Radioactive materials L-[2,3,4,5,6-^{3}H]phenylalanine and [α-^{32}P]ATP were from Amersham Biosciences. AMV reverse transcriptase, dNTPs and ddNTPs were obtained from Roche Diagnostics. N^1-azidobenzamidino (ABA)-spermine was synthesized and purified according to Clark *et al.* (1991).

4.2. Biochemical preparations

70S Ribosomes were isolated from *E. coli* K12 cells, as described previously (Xaplanteri *et al.* 2005). Ac[^{3}H]Phe-tRNA charged to 85% and complex C carrying Ac[^{3}H]Phe-$tRNA^{Phe}$ at the P-site and $tRNA^{Phe}$ at the E-site were prepared in buffer A (100 mM Tris.HCl, pH 7.2, 4.5 mM magnesium acetate, 150 mM ammonium chloride, and 6 mM 2-mercaptoethanol) and purified as shown elsewhere (Dinos et al. 2004). Whenever desired, 100 μM spermine was also included in buffer A. The percentage of complex C, reactive towards puromycin, was >90%.

Complex C was photolabeled with 100 μM ABA-spermine in HEPES buffer containing 4.5 mM Mg^{2+} and 150 mM NH_4^+, and separated from excess photoprobe, as shown previously (Xaplanteri et al. 2005).

4.3. Time-resolved binding of clindamycin to complex C

Complex C (10 pmol), untreated or photolabeled with 100 μM spermine, was incubated in the absence or presence of 55 μM clindamycin ($10 \times K_i$) in 100 μL buffer B [50 mM HEPES/KOH, pH 7.2, 4.5 mM $Mg(CH3COO)_2$, 150 mM NH_4Cl, and 5 mM dithiothreitol] at 25 °C, either for 1 s (CI probing) or for 1 min (C*I probing). In another series of experiments, 100 μM spermine was included in the reaction buffer, when untreated complex C was used as target of clindamycin. Probing of CI and C*I complexes with DMS and kethoxal, and monitoring of the modifications in 23S rRNA were performed by primer extension analysis, according to Stern et al. (1988). The primers were complementary to the sequences 2099-2116 and 2561-2578 of 23S rRNA. The cDNA products were run on 6% polyacrylamide/7 M urea gels. The positions of modified nucleotides were identified with reference to sequencing reactions performed on an unmodified rRNA template. Band intensities were quantified by phosphorimaging (Fujifilm, FLA-3000, Berthold; Image Quant Software AIDA, Raytest) and averaged over three replications. The variability between lanes was corrected using the relative intensity of a band corresponding to a nucleotide whose accessibility to the chemical probe was not affected by the drug binding.

4.4. Clindamycin-ribosome modeling

Flexible docking of clindamycin into the binding pocket of the 50S ribosomal subunit from *E. coli* (PDB: 3OFZ) was performed using the program AutoDock Vina (Trott and Olson 2010). A- and P-site bound Phe-tRNAs from *T. thermophilus* (PDB: 2WDK) were introduced in the model, after structural alignment of *E. coli* and *T. thermophilus* 50S ribosomal subunits using the program VMD (Humphrey et al. 1996). Two different starting conformers of clindamycin were applied; one obtained by crystallography in an *E. coli* ribosome-clindamycin complex (Dunkle et al. 2010), and a second one taken from a ribosome-clindamycin complex of *D. radiodurans*, having the pyrrolidinyl propyl group rotated by 180° (Schlünzen et al. 2001). Figure 4 was visualized, using the program VMD.

References

Agmon H, Amit M, Auerbach T, Bashan A, Baram D, Bartels H, Berisio R, Greenberg I, Harms J, Hansen HAS, Kessler M, Pyetan E, Schluenzen F, Sittner A, Yonath A, Zarivach R (2004) Ribosomal crystallography: a flexible nucleotide anchoring tRNA translocation, facilitates peptide-bond formation, chirality discrimination and antibiotic synergism. FEBS Lett 567: 20–26.

Bashan A, Agmon I, Zarivach R, Schluenzen F, Harms J, Berisio R, Bartels H, Franceschi F, Auerbach T, Hansen HA, Kossoy E, Kessler M, Yonath A (2003) Structural basis of the ribosomal machinery for peptide bond formation, translocation, and nascent chain progression. Mol Cell 11: 91–102.

Celma ML, Monro RE, Vázquez D (1971) Substrate and antibiotic binding sites at the peptidyl transferase centre of *E. coli* ribosomes: Binding of UACCA-Leu to 50 S subunits. FEBS Lett 13: 247–251.

Černá J, Rychlík I (1972) The effect of antibiotics on the substrate binding to the acceptor and donor site of ribosomal peptidyltransferase of an erythromycin-resistant mutant of *Escherichia coli*. Biochim Biophys Acta 287: 292–300.

Cheney BV (1974) Ab initio calculations on large molecules using molecular fragments. Structural correlations between natural substrate moieties and some antibiotic inhibitors of peptidyl transferase. J Med Chem 17: 590–599.

Clark E, Swank RA, Morgan JE, Basu H, Matthews HR (1991) Two new photoaffinity polyamines appear to alter the helical twist of DNA in nucleosome core particles. Biochemistry 30: 4009–4020.

Dinos G, Wilson DN, Teraoka Y, Szaflarski W, Fucini P, Kalpaxis DL, Nierhaus KH (2004) Dissecting the ribosomal inhibition mechanisms of edeine and pactamycin: the universally conserved residues G693 and C795 regulate P-site RNA binding. Mol Cell:13, 113–124.

Douthwaite S (1992) Interaction of the antibiotics clindamycin and lincomycin with *Escherichia coli* 23S ribosomal RNA. Nucleic Acids Res 20: 4717–4720.

Dunkle JA, Xiong U, Mankin AS, Cate JHD (2010) Structures of the *Escherichia coli* ribosome with antibiotics bound near the peptidyl transferase center explain spectra of drug action. Proc Natl Acad Sci USA 107: 17152–17157.

Fitzhuge AL (1998) Antibiotic inhibitors of the peptidyl transferase center. 1. Clindamycin as a composite analogue of the transfer RNA fragments L-Pro-Met and the D-ribosyl ring of adenosine. Bioorg Med Chem Lett 8: 87–92.

Fabbretti A, Milon P, Giuliodori AM, Gualerzi CO, Pon CL (2007) Real-time dynamics of ribosome-ligand interaction by time-resolved chemical probing methods. Methods Enzymol 430: 45–58.

Humphrey W, Dalke A, Schulten K (1996) VMD-Visual molecular dynamics. J Mol Graphics 14: 33–38.

Kallia-Raftopoulos S, Kalpaxis DL, Coutsogeorgopoulos C (1994) New aspects of the kinetics of inhibition by lincomycin of peptide bond formation. Mol Pharmacol 46: 1009–1014.

Kehrenberg C, Schwarz S, Jacobsen L, Hansen LH, Vester B (2005) A new mechanism for chloramphenicol, florfenicol and clindamycin resistance: methylation of 23S ribosomal RNA at A2503. Mol Microbiol 57: 1064–1073.

Kouvela EC, Petropoulos AD, Kalpaxis DL (2006) Unraveling new features of clindamycin interaction with functional ribosomes and dependence of the drug potency on polyamines. J Biol Chem 281: 23103–23110.

Menninger JR, Coleman RA (1993) Lincosamide antibiotics stimulate dissociation of peptidyl-tRNA from ribosomes. Antimicrob Agents Chemother 37: 2027–2029.

Moazed D, Noller HF (1989) Interaction of tRNA with 23S rRNA in the ribosomal A, P, and E sites. Cell 57: 585–597.

Morrison JB, Walsh CT (1988) The behavior and significance of slow-binding enzyme inhibitors. Adv Enzymol Relat Areas Mol Biol 61: 201–301.

Poehlsgaard J, Pfister P, Böttger EC, Douthwaite S (2005) Molecular mechanisms by which rRNA mutations confer resistance to clindamycin. Antimicrob Agends Chemother 49: 1553–1555.

Roberts MC (2008) Update on macrolide-lincosamide-streptogramin, ketolide, and oxazolidinone resistance genes. FEMS Microbiol Lett 282: 147–159.

Schlünzen F, Zarivach R, Harms J, Bashan A, Tocilj A, Albrecht R, Yonath A, Franceschi F (2000) Structural basis for the interaction of antibiotics with the peptidyl transferase centre in eubacteria. Nature 413: 814–821.

Stern S, Moazed D, Noller HF (1988) Structural analysis of RNA using chemical and enzymatic probing monitored by primer extension. Methods Enzymol:164, 481–489.

Tenson T, Lovmar M, Ehrenberg M (2003) The mechanism of action of macrolides, lincosamides and streptogramin B reveals the nascent peptide exit path in the ribosome. J Mol Biol 330: 1005–1014.

Triman KL (1999) Mutational analysis of 23S ribosomal RNA structure and function in *Escherichia coli*. Adv Genet 41: 157–195.

Trott O, Olson AJ (2010) AutoDock Vina: improving the speed and accuracy of docking with a new scoring function, efficient optimization and multithreading. J Comput Chem 31: 455–461.

Tu D, Blaha G, Moore PB, Steitz TA (2005) Structures of MLS_BK antibiotics bound to mutated large ribosomal subunits provide a structural explanation for resistance. Cell 121: 257–270.

Verdier L, Bertho G, Gharbi-Benarous J, Girault J (2000) Lincomycin and clindamycin conformations. A fragment shared by macrolides, ketolides and lincosamides determined from TRNOE ribosome-bound conformations. Bioorg Med Chem 8: 1225–1243.

Vogel Z, Vogel T, Zamir A, Elson D (1971) Correlation between the peptidyl transferase activity of the 50S ribosomal subunit and the ability of the subunit to interact with antibiotics. J Mol Biol 60: 339–346.

Xaplanteri MA, Petropoulos AD, Dinos GP, Kalpaxis DL (2005) Localization of spermine binding sites in 23S rRNA by photoaffinity labeling: parsing the spermine contribution to ribosomal 50S subunit functions. Nucleic Acids Res 33: 2792–2805.

Youngman EM, Brunelle JL, Kochaniak AB, Green R (2004) The active site of the ribosome is composed of two layers of conserved nucleotides with distinct roles in peptide bond formation and peptide release. Cell 117: 589–599.

Wilson DN (2009) The A-Z of bacterial translation inhibitors. Crit Rev Biochem Mol Biol 44: 393–433.